Phase behavior and lyotropic-liquid crystal structure of alkyltrimethylammonium bromide–water mixtures around freezing temperature of water[1]

Kazuhiro Fukada*, Yasuhiro Matsuzaka, Masatoshi Fujii, Tadashi Kato, Tsutomu Seimiya

Department of Chemistry, Faculty of Science, Tokyo Metropolitan University, Hachiohji, Tokyo 192-03, Japan

Abstract

Freezing and melting behaviors of concentrated cationic surfactant–water binary systems were investigated by using differential scanning calorimetry and polarized light microscopy, and the phase diagrams around the freezing temperature of water were constructed. The surfactants studied were decyl- and octyl-trimethylammonium bromide (abbreviated as DeTAB and OTAB). The OTAB–water system forms a lyotropic-liquid crystal in highly concentrated region of ca. 80 wt% OTAB. The head groups of OTAB strongly interact with water molecules and reduce freezing point of water down to $-33°C$. To clarify the structure of the liquid–crystalline phase, small angle X-ray diffraction study was carried out on DeTAB–water system as a function of composition at various temperatures. The observed diffraction patterns indicate the formation of the hexagonal phase, H_α, and suggests that the H_α phase consists of finite cylinder micelles with length increasing with surfactant content. © 1998 Elsevier Science B.V.

1. Introduction

Surfactant–water binary solutions have attracted a lot of attentions of colloid chemists, physical chemists, and biochemists as a typical self-assemble organized solution system. There have been many theoretical and experimental studies as far as the thermodynamic aspects of surfactant–water system are concerned, however, they are mostly related to the dilute micellar solution [1–3]. The studies on the highly concentrated solutions are rather scarce in

contrast. Thermal analysis of surfactant–water systems covering a wide range of concentration were carried out by Kodama et al., which revealed the important role of water in phase transition behaviors [4,5]. Also, we have reported the water vapor pressure data for ionic surfactant–water systems in the highly concentrated region where lyotropic-liquid crystal phase was formed [6].

In the present study, the freezing/melting behavior of cationic surfactant (alkyltrimethylammonium bromide)–water systems was investigated in the concentrated regions by using differential scanning calorimetry (DSC), expecting that ice formation would provide insight into the nature of dehydration of lyotropic-liquid crystals. Several reports about freezing and melting of water in ionic surfactant–

---

*Corresponding author. Fax: +81 426 77 2525; e-mail: fukada-kazuhiro@c.metro-u.ac.jp

water or lipid–water systems have been reported in this context [7–9]. The small angle X-ray diffraction for DeTAB–water system was also investigated. The X-ray data were informative to know the structural feature of the lyotropic liquid–crystalline phase.

2. Experimental

2.1. Materials

A guaranteed grade reagent of decyltrimethylammonium bromide and octyltrimethylammonium bromide (abbreviated as DeTAB and OTAB, respectively; Tokyo Kasei) were used after recrystallized twice from acetone/ethanol mixture and dried in vacuo. Sample mixtures prepared gravimetrically by using water purified with Milli-Q Lab (Millipore) were sealed in glass tubes and equilibrated in a hot-water (ca. 90°C) to ensure homogeneous mixing.

2.2. Polarized light microscopy

A polarizing microscope (BHSP, Olympus) equipped with a heating/cooling stage (FP82HT, Mettler) was used to observe the texture of sample mixtures during heating/cooling process.

2.3. Differential scanning calorimetry (DSC)

DSC measurements were carried out with a Seiko-Denshi DSC220C. Sample mixtures (ca. 10 mg) in a silver pan were cooled down from 20°C to −50°C for DeTAB (or to −80°C for OTAB) at a cooling rate of 1–2°C/min and then heated up to 10°C at a rate of 0.5°C/min. Annealing procedure by heating and cooling cycle in the above temperature range did not affect the DSC curves.

2.4. X-ray diffraction

Small angle X-ray diffraction was measured by a high-resolution small angle X-ray scattering instrument equipped with a tungsten/silicon multilayer monochromator and a self-rotating anode system [10]. Monochromatic CuKα1 radiation (λ=0.15405 nm) from a rotating anode (SRAMXP18, Mac Science) operated at 45 kV and 400 mA was

focused by the Kratky slit and introduced to the sample. The diffracted X-rays were detected by the digital imaging plate (DIP200, Mac Science) over a range of scattering vectors, $Q=4\pi\sin\theta/\lambda$, where 2θ is the scattering angle: $0.02<Q<0.4$ Å^{-1}. Since Kratky slit optics is employed in the instrument, slit correction for the intensity distribution along the length of the incident X-ray beam was necessary for quantitative analysis. We used the slit correction method proposed by Vonk [11]. The temperature of samples, which were mounted to a 1 mm-thick cell, was controlled by using the thermostated cell holder.

3. Results and discussion

3.1. Differential scanning calorimetry

Fig. 1 shows the DSC heating curves for DeTAB–water and OTAB–water systems over a wide concentration range. For DeTAB–water mixtures (Fig. 1(a)), only one endothermic peak at −13°C was observed during heating process when content of surfactant was above 70 wt%. In the composition range of 56–70 wt%, an addition peak around −3°C emerged and its peak area increased with water content. When content of DeTAB became lower than 56 wt%, the third endothermic peak appeared around −2°C. During cooling process, the super-cooled exothermic peaks corresponding to the endothermic peaks were detected as shown in Fig. 2(a).

For OTAB–water mixtures (Fig. 1(b)), three endothermic peaks appeared eventually one after
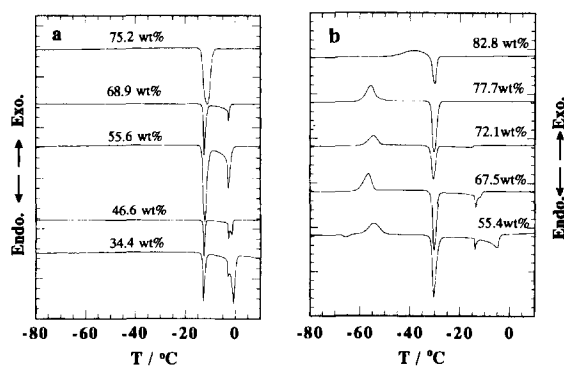

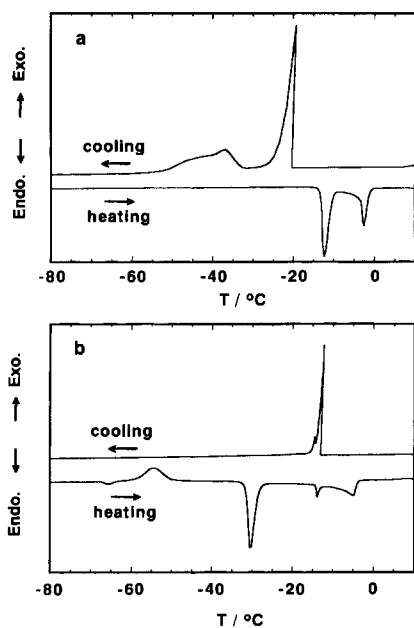Fig. 1. DSC heating curves of DeTAB–water (a) and OTAB–water (b) systems with various surfactant content.

Fig. 2. DSC cooling and heating curves of 55.6 wt% DeTAB (a) and 55.4 wt% OTAB (b).
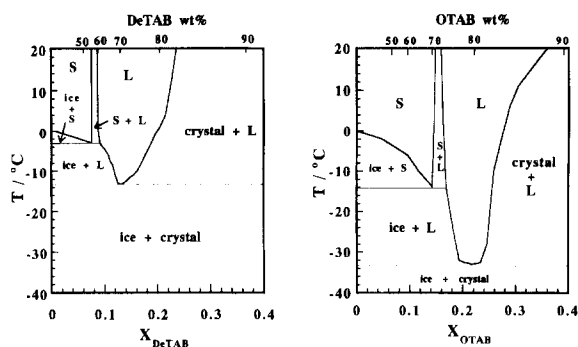

Fig. 3. Phase diagrams of DeTAB–water (left) and OTAB–water (right) systems. The characters S and L indicate isotropic micellar solution and lyotropic-liquid crystal phase, respectively.

another with the decrease of surfactant content in the similar way to DeTAB–water in a lower temperature region. When OTAB content was above 72 wt%, one endothermic peak at −33°C was observed. For samples of 60–72 wt% OTAB (or <60 wt% OTAB), the additional endothermic peak(s) at −14°C (and around −5°C–0°C) was detected. The interesting observation for OTAB–water mixture is that a broad exothermic peak around −55°C was detected as shown in Fig. 1(b). Also, the exothermic peak corresponding to the endothermic peak at −33°C was not observed during cooling process (see Fig. 2(b)). The cause for the phenomena is discussed in the following subsection. It is to be noted here that similar thermal behavior with exo- and endo-thermic peaks on heating has been reported for the frozen aqueous LiCl solutions (15 and 17 mol kg^{-1}) [12].

3.2. Phase diagram

By the observation with the naked eye and polarizing light microscope, and the X-ray diffraction patterns of DeTAB–water and OTAB–water mixtures with various composition, freezing temperature, phase separation composition, and the crystallization temperature of solute were determined. Based on those data, phase diagrams of DeTAB–water and OTAB–water binary systems were constructed as shown in Fig. 3. Comparing Fig. 3 to the DSC heating curves (Fig. 1), we can see that the temperatures of the endothermic peaks during heating process in DSC correspond to the following phase transition temperatures; (1) separation of lyotropic-liquid crystalline phase ("L"-phase in Fig. 3) from the mixture of surfactant crystal+co-existing ice (−13°C for DeTAB and −33°C for OTAB), (2) phase transition from "L" to micellar solution, "S", (−3°C for DeTAB and −14°C for OTAB), and (3) melting of the ice which co-existed with micellar solution (around 0°C).

When the mole fraction of OTAB (X_{OTAB}) is above 0.2, i.e., above 77 wt% OTAB, the ice formed by cooling below −33°C may not be an ordinary ice with the ordered crystal structure but a sort of amorphous since no exothermal DSC peak corresponding to the endothermic peak at −33°C in the heating process was observed in the cooling process. It is likely that undetected glass transition might occur in the cooling process, and the structural relaxation from the unstable amorphous state to the thermodynamically stable state proceeded around −55°C to give the broad exothermal peak during heating process.

Comparing the phase diagram of OTAB–water with that of DeTAB–water, one can see that the one phase liquid–crystalline region of OTAB shifts to higher mole fraction than DeTAB and extends to lower temperature. So, we may say that water molecules

in the highly concentrated liquid–crystalline phase of OTAB strongly bind to the head group of OTAB and resist freezing. In DeTAB–water system, on the other hand, the crystal of DeTAB separates when the mole fraction exceeds 0.14 (0.22) at $-13°C$ (20°C) because the hydrophobic interaction between decyl groups of DeTAB is stronger than that between octyl groups of OTAB.

Phase diagram for dodecyltrimethylammonium chloride (DTAC)–water system has been reported in wide temperature and composition range [13,14]. The temperature and composition range of the one-phase lyotropic-liquid crystal region was similar to that of DeTAB–water, however, which was divided into cubic and hexagonal liquid–crystalline phase around $X_{DTAC}=0.08$.

3.3. Thermodynamic nature of water in the lyotropic-liquid crystal

Considering the strength of hydration in the liquid–crystalline state, it may be worth to review our previous data on water vapor pressure for the aqueous surfactant systems. For the measurement of the equilibrium vapor pressure of concentrated aqueous surfactant systems, we had employed a diaphragm type variable capacitance manometer. (The details of the experiment are given in Ref. [6].) Since the vapor pressure of the surfactants themselves was small enough to be ignored, the measured pressure was regarded to be that of water. The activity of water (a) was calculated from the vapor pressure of the system (P); $a=P/P_0$, where P_0 is the vapor pressure of pure water.

In Fig. 4, the activity of water calculated from the vapor pressure of DeTAB–water and OTAB–water mixtures was indicated as a function of mole fraction of the surfactant, X_s. Below the heterogeneous region of high X_s where the activity of water is constant, the system is either lyotropic-liquid crystal or micellar solution. The positive deviation from Raoult line (which linearly decreases with the surfactant content) is shown in the composition range of $X_s<0.15$, which is one of the features of the "organized solution" [15]. The activity of water steeply falled-off when OTAB formed lyotropic-liquid crystal $(X_s>0.18)$, which is another evidence of strong interaction between OTAB and water in the liquid–crystalline state.
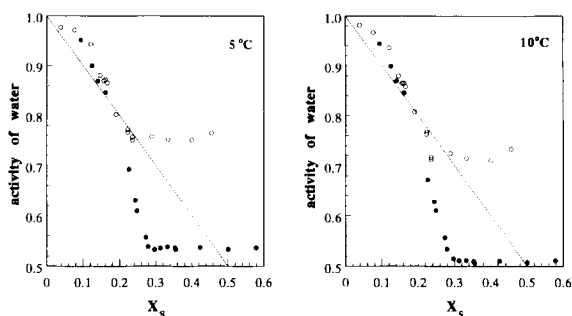

Fig. 4. Activity of water as a function of mole fraction of surfactant, X_s, for DeTAB–water ($\bigcirc$) and OTAB–water ($\bullet$) at 5°C and 10°C. Raoult line is indicated by the solid line with slope of -1. Adapted from Ref. [6].
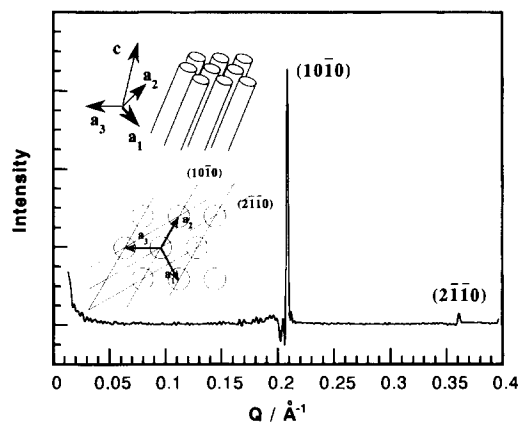

Fig. 5. The typical small angle X-ray diffraction pattern observed for lyotropic-liquid crystalline phase of DeTAB; 66.4 wt% DeTAB at 25°C. Inset: Schematic drawing of the hexagonal phase, 3-D image and 2-D image viewed along $\langle 0001 \rangle$ direction.

3.4. Structure of lyotropic-liquid crystalline phase of DeTAB–water system

The typical small angle X-ray diffraction pattern observed for the liquid–crystal of DeTAB is shown in Fig. 5. Two diffraction peaks were characterized by the spacing of planes in the ratio $1:\sqrt{3}$ indicating that DeTAB formed hexagonal liquid–crystal phase, H_α, and the peaks are indexed as $(10\bar{1}0)$ and $(2\bar{1}\bar{1}0)$, respectively. The structure of H_α phase had been assumed to consist of infinite cylinder micelles with a two-dimensional positional order in the plane perpendicular to the cylinder axes as shown in the inserted illustration of Fig. 5. However, an alternative model for H_α phase based on cylinder micelles with

finite length that may change with composition was proposed for sodium dodecyl sulfate–water and potassium oleate–water systems [16,17]. The absence of diffraction in the direction perpendicular to the hexagonal plane was ascribed to polydispersity of micellar length. To decide which model fits better for our system, composition dependence of the hexagonal unit-cell parameter was interpreted according to the procedure of Amaral et al. [17] with slight modifications as follows.

Let us consider an hexagonal array of cylinder micelles with radius R, length L, and an average distance C between micellar center in the direction of cylinder axis. The volume fraction of surfactant, ϕ_v, must be the same in the unit cell as in the whole system. Therefore,

$$\phi_v = (L/C)(2\pi R^2)/(\sqrt{3}\underline{a}^2) \qquad (1)$$

where $\underline{a}$ is the hexagonal unit-cell parameter. Since this treatment considers a constant density for both paraffinic and polar moieties of the micelles as usual, R would be constant irrespective of the composition. Furthermore, if we assume the infinite cylinder micelle, then $L=C$, and we get

$$\underline{a} \propto \phi_v^{-1/2}. \qquad (2)$$

Fig. 6 shows the composition dependence of $(10\bar{1}0)$ peak of DeTAB liquid-crystal, and the hexagonal unit-cell parameter, $\underline{a}$, is calculated from the peak position; $\underline{a} = 4\pi/(\sqrt{3}Q)$. Fig. 7 shows the obtained variation of the hexagonal parameter with DeTAB concentration,
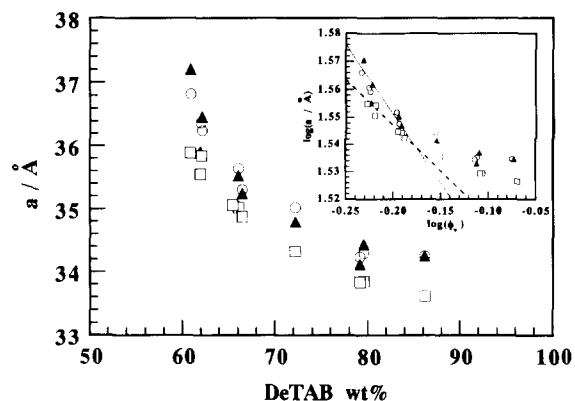
Fig. 7. Hexagonal unit-cell parameter, $\underline{a}$, as a function of surfactant content for DeTAB–water system at 5°C (○), 10°C (▲) and 25°C (□). Inset: log–log plot of $\underline{a}$ vs. volume fraction ϕ_v of DeTAB micelle in the hexagonal phase. Solid and broken lines indicate the slope −1/2 and −1/3, respectively.

and the inset is the log–log plot of $\underline{a}$ vs. volume fraction ϕ_v calculated using values 0.918 (5°C), 0.922 (10°C), and 0.933 cm³/g (25°C) for partial specific volume of DeTAB micelle [18] and the literature values of water specific volume at each temperature. We can see that the exponent of Eq. (2) fits the data at 5°C and 10°C in the composition range <70 wt%, but the data at 25°C were rather fitted by the exponent −1/3. If we assume finite objects like spherocylinder with volume around the objects decreasing in all three dimensions, the exponent should be −1/3 instead of −1/2. In the highly concentrated region (>70 wt% DeTAB), however, the gentle slope of the data points cannot be fitted by both −1/2 and −1/3 exponent. These results suggest that the H_α phase of DeTAB consists of finite cylinder micelles and the cylinder length increases with the surfactant content when the concentration exceeds 70 wt%. By considering the growth of cylinder length L with concentration, which leads to the decrease of amount of water occupying positions along the cylinder lengths, it is expected that the amount of water between the cylinder lengths does not decrease so much. In this way the hexagonal unit-cell parameter may give the gentle slope as shown in Fig. 7 in the concentrated region.

For DeTAB liquid crystal (73.0 wt% DeTAB), we further examined the variation of X-ray diffraction when the sample was cooled from 25°C to −30°C and then heated back to 25°C (see Fig. 8). It is clear that the peak position of $(10\bar{1}0)$ diffraction shifts to lower
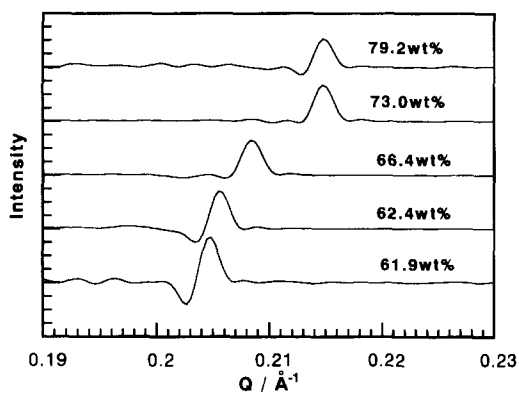

Fig. 6. The X-ray diffraction from $(10\bar{1}0)$ plane of liquid–crystal of DeTAB with various surfactant content at 25°C.
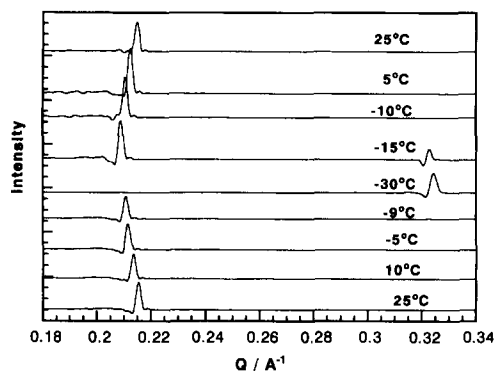
Fig. 8. Variation of small angle X-ray diffraction of DeTAB–water system (73 wt% DeTAB) by cooling and heating. The uppermost curve is the initial diffraction pattern at 25°C. The lower curves indicate the diffraction pattern observed during cooling process (25°C→−30°C) and heating process (−30°C→25°C).

Q, i.e., larger a, with decrease of temperature. This peak shift may be interpreted by the axial growth of the hexagonal phase surfactant cylinders by cooling. At −15°C and −30°C, the diffraction peak for DeTAB crystal ($Q{\approx}0.325$ Å^{-1}) was observed, which is consistent with the phase diagram in Fig. 3.

For OTAB–water systems, the observed X-ray diffraction patterns from the liquid–crystal phase were rather complicated and changed with composition and temperature. The assignment of the liquid–crystal structure is in progress and will appear in a future paper.

Acknowledgements

References

[1] C. Tanford, The Hydrophobic Effect, chap. 6–9, 2nd ed., Wiley, New York, 1980.

[2] J.N. Israelachvili, Intermolecular and Surface Forces, chap. 16–17, 2nd ed., Academic, London, 1991.

[3] Y. Moroi, Micelles: Theoreties and Applied Aspects, Plenum, New York, 1992.

[4] M. Kodama, S. Seki, J. Colloid Interface Sci. 117 (1987) 485.

[5] M. Kodama, K. Tsujii, S. Seki, J. Phys. Chem. 94 (1990) 815.

[6] K. Fukada, Y. Matsuzaka, Y. Ito, T. Nakazato, K. Matsui, Y. Hosoi, M. Fujii, T. Kato, T. Shirakawa, T. Seimiya, Colloid Polym. Sci. 271 (1993) 1197.

[7] M. Kodama, H. Hashigami, S. Seki, J. Colloid Interface Sci. 117 (1987) 497.

[8] A.S. Ulrich, M. Sami, A. Watts, Biochim. Biophys. Acta 1191 (1994) 225.

[9] J.T. Gleeson, S. Erramilli, S.M. Gruner, Biophys. J. 67 (1994) 706.

[10] H. Yoshida, T. Kato, K. Sakamoto, T. Murata, Memoirs Fac. Engineer. Tokyo Met. Univ. 44 (1994) 173.

[11] C.G. Vonk, J. Appl. Cryst. 4 (1971) 340.

[12] T. Hasebe, R. Tamamushi, K. Tanaka, J. Chem. Soc. Faraday Trans. 88 (1992) 205.

[13] G. Wikander, P.-O. Eriksson, E.E. Burnell, G. Lindblom, J. Phys. Chem. 94 (1990) 5964.

[14] G. Laughlin, in: D.N. Rubingh, P.M. Holland (Eds.), Cationic Surfactants: Physical Chemistry, surfactant science series, Vol. 37, Dekker, New York, 1991, p. 15.

[15] K. Shinoda, J. Phys. Chem. 89 (1985) 2429.

[16] R. Raymond, M. Wood, M.P. McDonald, J. Chem. Soc. Faraday Trans. 1(81) (1985) 273.

[17] L.Q. Amaral, A. Gulik, R. Itri, P. Mariani, Phys. Rev. A 46 (1992) 3548.

[18] R. De Lisi, C. Ostiguy, G. Perron, J.E. Desnoyers, J. Colloid Interface Sci. 71 (1979) 147.